Design Modifications and Thermal Analysis of Visco-Dampers for Extending Silicone Oil Durability

Márk Venczel[1], Michael Steidl[2], Árpád Veress[1,3]

[1]Budapest University of Technology and Economics, Faculty of Transportation Engineering and Vehicle Engineering, Department of Aeronautics and Naval Architecture, Műegyetem rkp. 3, H-1111 Budapest, Hungary
e-mail: mvenczel@vrht.bme.hu
[2]Hasse und Wrede, Georg-Knorr-Straße 4, 12681 Berlin, Germany
e-mail: Michael.Steidl@hassewrede.de
[3]Knorr-Bremse R&D Center Budapest, Engineering Calculations, Major u. 69, H-1119 Budapest, Hungary
e-mail: Arpad.Veress@knorr-bremse.com

Abstract: The application of torsional vibration dampers is reasonable in every internal combustion engine with high performance output, where the unbalanced gas and inertial forces cause harmful torsional oscillations on the crankshaft. These oscillations can lead to the fatigue and damage of engine components. A visco-damper is a type of torsional vibration damper. Temperature represents one of the highest effects, on the lifetime of its operational fluid, in this case, silicone oil. Design solutions are proposed and realized for increasing cooling capabilities and the durability of the silicone oil. The heat transfer processes inside and outside of the damper are determined by coupled fluid dynamics and heat transfer simulations. The plausibility of the results is confirmed by using a modified version of the Iwamoto equation. A temperature-based lifetime prediction method has been used for determining the lifespan of the synthetic damping medium. The proposed geometrical modifications, decrease the level of the temperature distributions and thereby, improve the durability of the silicone oil.

Keywords: torsional vibration damper; silicone oil; design modifications; thermal and life-time management; CFD

1 Introduction

Nowadays, the Transportation and Vehicle industry are some of the most dynamically evolving sectors; significant amounts of research is going on, not only in the area of e-mobility – including autonomous driving [1] – and traffic safety [2] but in the field of structural mechanics, as well, to provide longer lifetimes and higher levels of reliability and availability for vehicle systems and components in present and future.

Amongst the many different structural parts, torsional vibration dampers are found in the piston engines with the aim of damping torsional vibration of the crankshaft. Torsional vibration dampers are widespread from maritime applications through sports cars to heavy-duty vehicles due to their simple construction, high degree of reliability and relatively long lifetime. Considering the development trends in the field of internal combustion engines (ICE), they would eventually become smaller with a requirement for higher power output leading to an increase in the load on torsional vibration dampers in the future. Due to this evolution, there is a certain need for accurate methodologies and analyses to simulate the damper's function, as well as the lifespan influencing factors to be able to design the most suitable damper for any type of engine application. This is especially important for viscous torsional vibration dampers or shortly visco-dampers, which use silicone oil as operational fluid. The temperature is one of the most dominant factors for influencing its durability. Conducting thermal analysis on the silicone film situated inside the visco-damper poses a challenge as there are no practical and real time reliable techniques available so far. However, numerical methods – catering to the complex geometry and multidisciplinary physics – provide a plausible range of thermal distribution and can be replicated for various designs and their modifications.

This article provides an insight into the research and development process of visco-dampers, utilizing the relationship between the temperature of the silicone oil during operation and its effect on service life. Two different visco-damper geometries are considered in the presented analysis, both being in their early design phase.

1.1 Torsional Vibration Dampers

According to Figure 1, as the fuel burns in the piston cylinders of an ICE (1), thermal energy is released and converted into mechanical load (torque) by connecting rods (2) on the crankshaft (3). The continuous repetition of momentary angular acceleration (determined by the ignition and injection sequence) causes irregular and periodic oscillations on the shaft and significant mechanical stresses in the drivetrain. These oscillations are responsible for noise, higher stresses and ultimately, engine failure. Fatigue occurs when the frequency of the oscillation corresponds to the natural frequency of the crankshaft and driven components. [3] [4]

To prevent this failure and reduce the amplitude of vibration, a torsional vibration damper (4) can be mounted onto the free-end of the crankshaft or integrated into the flywheel (5). Several types of torsional vibration damper are available such as frictional, spring, rubber and viscous [3].

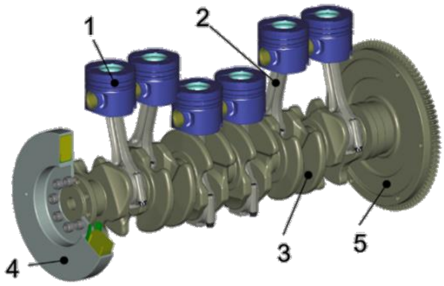

Figure 1
Torsional vibration damper mounted on the free-end of crankshaft [3]

Visco-dampers are some of the simplest devices, in damping technology. They consist of a closed annular space, called a housing, with a freely moving inertia ring within it as seen in Figure 2 (left). The inertia ring is guided by polymer slide bearings and surrounded by a thin film of damping medium. Regarding the operation of the device, the damping effect can be explained as follow. In the case of undisturbed rotation of the crankshaft without superposed oscillations, the inertia ring rotates together with the housing without any slip. With the onset of torsional oscillations, a relative motion between the housing and the ring occurs, which causes tangential shear stress in the damping medium. The damping effect is the sum of the shear stresses developing on the friction surfaces between the housing and the ring. Silicone oil is a non-Newtonian fluid and it has a different response to external forces compared to other conventional (Newtonian) fluids. Because of this characteristic, the relative velocity between the housing and the inertia ring influences the viscosity and thus the damping characteristics of the oil. During operation, the damping fluid is exposed to high thermal load originating from the friction and shear of the oil layer and from the engine and surrounding air as heat sources. The viscosity of the silicone oil varies with the change in temperature, thus cooling fin plates may be mounted onto the housing or onto the cover in one or two rows (see Figure 2 (right)) to keep the operational temperature within the designed range. [3] [5]

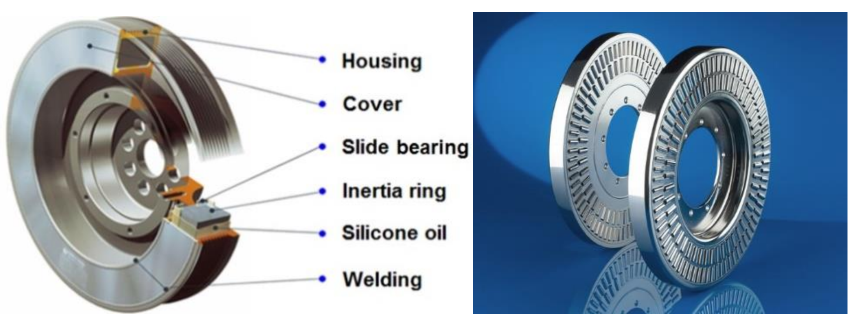

Figure 2
Structure of a visco-damper (left) [3] and cooling fins in two rows on the damper (right) [6]

There has been much research in conjunction with torsional vibration dampers in recent times. Homik [7] investigated the torsional and longitudinal vibrations of crankshafts of vessels and discussed the possibilities for vibration damping thoroughly. The characteristics of shaft amplitudes for rubber and viscous type of torsional vibration damper were analyzed and compared through resonance measurements.

Do-Kwan et al. [8] in their study provided an insight into the multidisciplinary design process of vibration dampers, in which a visco-damper for high performance crankshaft system of a transporting machine was developed by using reverse engineering, structural stability analysis and manufacturing techniques. Several prototypes were made with inertia rings of different sizes and masses and profound performance tests were conducted.

Damping properties play an important role in the determination of dynamic response of a crankshaft and a visco-damper however, these damping parameters are very scarce and cannot be deduced deterministically from other structural properties. Thus, experiments must be conducted on complete devices of similar characteristics. One such parameter is the damping coefficient. In the work of Navale et al. [9] a test rig was developed to find out the damping coefficient of a viscous damper. The verification of the experimental results was performed by comparing them with analytical results. The damping coefficient (obtained from the test setup) can be used to check the quality and the usage of a damper with ease.

A different type of torsional vibration damper – known as magnetorheological damper – has been recently investigated. This damper is filled with magnetorheological fluid (MRF), which is controlled by a magnetic field generated by an electromagnet. As the intensity of the electromagnet increases, the viscosity of fluid changes (increases) as well. Ehab et al. [10] developed a hybrid torsional vibration damper incorporating conventional centrifugal pendulum absorber and magnetorheological damper and demonstrated the superior performance of the proposed design. More details can be found about MRF technology for visco-dampers in Anant et al.'s work [11].

1.2 Silicone Oils for Torsional Vibration Damping

Silicone oils belong to the silicon-based lubricants and include every type of polymerized liquid siloxane, in which the molecules contain organic side chains. [12] Polydimethylsiloxane (PDMS) is a special type of silicone oil, which is one of the most suitable materials for visco-dampers due to its favorable tensile strength, density and low friction properties. It mitigates efficiently the unwanted oscillations in a wide frequency range. Its chemical formula is $(H_3C)_3[Si(CH_3)_2O]_uSi(CH_3)_3$ where u is the number of repeating monomer units. The higher this number, the higher is the viscosity of the oil sample. [13]

Today, the viscous behavior of the silicone oils has been well studied and is relatively well understood. Czirják and Kőkuti [14] [15] made efforts to describe the non-linear viscoelasticity and thixotropy of silicone oils in mathematical way and they created different rheological models for research and development purpose.

Several scientific researches deal with thermal and material stability, improvements and the response of PDMS molecular structure to high temperature. As it turned out from the study of Camino et al. [16] [17], thermal volatilization and weight loss of PDMS oil occurs during a molecular mechanism at lower temperature with formation of cyclic oligomers through Si-O backbone scission. This kind of decomposition of the investigated material is directly proportional to the rate of heat increase that takes place and is determined by the diffusion and evaporation of produced oligomers following first order Arrhenius behavior and having activation energy of ~ 27 kcal mol^{-1}. At higher temperatures, a radical mechanism occurs through homolytic $Si\text{-}CH_3$ bond scission followed by hydrogen abstraction and leads to the formation of methane. The flexibility of PDMS chain is reduced by the cross-linking of macro-radical groups and further splitting of cyclic oligomers is restricted. The oxidative cross-linking and the reorganization of split bonds improve the thermal stability of the material and produces ceramic silicon-oxycarbide.

Different methods were developed to improve the thermal stability and resistance of PDMS. Dongzhi et al. [18] for example described a way to enhance the properties by preparation of PDMS composites using polyvinyl silsesquioxanes (PVS) as reinforcing agent by hydrolytic condensation in the presence of organotin catalyst. Experimental results show that the thermal and mechanical properties of the novel composites were improved greatly by adding PVS and their resistance to thermal oxidation in nitrogen, increased as well. However, no differences, in the case of the air environment, were observed.

For damping applications, there are some uncertainties in the preliminary design phase of visco-dampers related to operation such as the rate of change of viscosity of PDMS oil in the damper, heat generated and dissipated, damping performance and the temperature distribution. In Wang et al.'s report [19] an engine-damper matching calculation method is introduced based on the heat equilibrium. The accuracy and the validation of the implemented calculation process were demonstrated by measurement results on a real diesel engine equipped with an operational visco-damper.

The present introductory chapter primarily dealt with an overview about the types, the structures and the general operation of torsional vibration dampers with a special focus on visco-ones. Background on the damping medium (in our case, silicone oil), the general effects of temperature change and the continuous research and development on increasing the operational temperature range were also discussed. However, in case of extreme operational conditions, where power dissipation and the ambient temperature both are high, a special design methodology is required to limit the oil temperature to tolerable values. Hence, a computational fluid dynamics-based (CFD) methodology has been introduced during the design phase of torsional visco-dampers to control the thermal degradation process and thus the service life of silicone oil.

1.3 Iwamoto Equation for Temperature Estimation

A half empirical analytical expression, developed by Shoichi Iwamoto, is applied for preliminary thermal analysis of viscous torsional vibration dampers to estimate the outer surface temperature of the damper housing under operation.

A modified version of the original Iwamoto Eq. (1.1) [5] is considered in the present case. The calculated value by the equation will be used in the plausibility analysis of the CFD results. The circumferentially averaged temperature distribution of the case will be compared with the results of the numerical analyses described in the forthcoming part of the article and conclusions are going to be drawn about the reliability of the analyses.

$$T_{case} = \frac{Q_{damp} - c \cdot A_{ring}}{d \cdot \left(-g \cdot \frac{D_0}{D_{ring}} + h\right) \cdot n_{case}^{k} \cdot \left(p \cdot A_{ring}\right)^{r}} + T_{ambient} \tag{1.1}$$

The parameters in Eq. (1.1) are next:

Q_{damp} is damping performance which converts into heat [W]; A_{ring} is inertia ring wetted surface [m^2]; n is crankshaft rotational speed [RPM]; D_0 is damper outer diameter [m]; D_{ring} is inertia ring inner diameter [m]; $T_{ambient}$ is ambient temperature [K]; c, d, g, h, k, p, r are Iwamoto parameters [-].

2 Degradation of Silicone Oil

The best method for monitoring the degradation of the silicone oil is determining the viscosity change. The viscosity is one of the most important properties of the damping media; it describes the degree of internal friction among the fluid layers, which in turn result energy loss.

Based on static degradation measurements, the viscosity and the lifespan of PDMS oil depend strongly on the operational temperature. The following technical factors can be considered to influence the operation of a torsional visco-damper: [20]

- Type of silicone oil (initial viscosity)
- Speed of rotation (damping performance)
- Gap-sizes between the housing and the inertia ring (gap-size investigation)

- Positioning of the cooling fins (cooling fin mounting investigation)

This paper investigates the effect of different gap-sizes and the side-positions of the cooling fin geometries on thermal load and on the service life of PDMS oil. It also considers the material aspects integrated into the lifetime of the oil discussed below. A theoretical variable, called Degradation Factor (*DF*), is introduced for lifetime calculations. *DF* provides information about the rate of change of viscosity of a given silicone oil under continuous thermal load at constant operational temperature for one day as shown by Eq. (2.1) [20]

$$DF = \frac{\eta_0 - \eta_1}{\eta_0} \cdot 100 \tag{2.1}$$

where *DF* is the degradation factor [%/day]; η_0 is the initial dynamic viscosity [Pa s] and η_1 is the changed dynamic viscosity after one day [Pa s].

Since *DF* is the function of the temperature [20], the temperature distribution in the damper, especially in the silicone oil, must be determined to calculate the degradation factor of the PDMS oil. The maximum change in viscosity allowed $\Delta\eta_{allowed}$ [%] can be calculated by Eq. 2.2 by using the values of the initial viscosity η_0 [Pa s] and the minimum allowed viscosity $\eta_{\min}$ [Pa s].

$$\Delta\eta_{allowed} = \frac{\eta_0 - \eta_{\min}}{\eta_0} \cdot 100 \tag{2.2}$$

As the degradation (considering in the range from the oil's initial state to the allowable degree of degradation state) is linear function of time, dividing the maximum change in viscosity allowed $\Delta\eta_{allowed}$ [%] by DF [%/day] will provide the service life $t_{service}$ [day] of the fluid as presented in Eq. 2.3.

$$t_{service} = \frac{\Delta\eta_{allowed}}{DF} \tag{2.3}$$

3 Design Methodologies, Numerical Analyses and Silicone Oil Durability

The enhancement of effectiveness in the vehicle industry is a general expectation, there are several innovative researches in this field [21] [22]. In the last decade, the attention of product development is focused more on technical modelling and simulation activity including CFD, which are becoming an essential part and a powerful tool for design, development and researches as it is shown by [23] and [24].

Bicsák et al. [25] used CFD techniques to introduce a minimum requirement demanding method for investigating the effect of an aircraft propeller in low Mach number flow regime. The results of Actuator Disk Method (ADM) with induced velocities and total pressure were compared to a reference solution generated by Rotating Domain Model (RDM). It turned out from the numerical investigation that ADM with total pressure boundary condition provides acceptably close results to RDM solution. In terms of computational time, ADM with total pressure boundary condition required less time by 95% to provide converged simulation results compared to RDM simulation.

Kátai et al. [26] performed CFD analysis on a novel mobile refrigerated container. The cooling air velocity distribution in empty and fully loaded cases was investigated while the shape of inlet air profile and the necessity of auxiliary ventilator installation were also tested. The outcome of the CFD calculation was supported by hydrodynamic experimental small-scale test. Both the CFD calculation and the experimental model proved the fact, that the original container design is not suitable for proper cooling due to the lack of generated air circulation. By applying multijet technology with auxiliary fans installed on bottom of the partition wall and directed evaporator blow-out, the quality of cooling can be improved.

CFD is an appropriate tool not only for investigating flow characteristics but to understand the combustion phenomena and pollution composition of an ICE as well. Akbarian et al. studied in their work [27] the effect of fuel combination (natural gas and diesel fuel) on the performance and emissions of a dual-fueled engine under constant speed with different loads. According to the results, the dual-fueled mode of the engine causes lower $CO2$, NOx and particle materials (PM) emission under all load conditions compared to the diesel mode. The authors suggest to use the engine in the dual mode at 30% and 50% of the pilot fuel (diesel) ratio in full and half loads respectively for significant reduction in emission and fuel consumption.

Fabio et al. [28] used CFD method for proposing and testing an alternative wall function model to calculate more reliable heat fluxes on the wall of high-performance spark ignition engines. Four currently produced and direct injection spark ignition turbocharged engines had been selected with different operating conditions for heat transfer model improvement purpose. Experimental engine thermal survey and point-wise temperature measurement data were used to validate their developed wall heat transfer model.

CFD enables also damper developers to better understand the complex fluid flow and the detailed thermal distribution inside a visco-damper during operation. ANSYS CFX commercial code has been used in this work for numerical modelling and analysis. The general conservation law for mass, momentum and energy are discretized into a system of algebraic equations. Time discretization is achieved by 'First or Second Order Implicit Backward Euler' scheme, which solves a multidimensional nonlinear algebraic equation in each iteration. The discretized system of algebraic equations is then determined numerically over the predefined control volumes through iteration steps with the 'Multigrid Accelerated Incomplete Lower Upper Factorization' technique to render the solution field. [29]

3.1 Geometry – Design Modifications for Lifetime Extension

As discussed in Chapter 2, the service life of silicone oil is heavily dependent on the temperature. The goal of the visco-damper developments is to design appropriate geometry in such a way that the operational temperature remains in favorable range, prolonging the lifetime of the lubricant. The temperature distribution of the oil can be influenced either by properly selected gap-sizes, which determine the amount of fluid and the film thickness between the moving components (housing and inertia ring) and by application of advanced cooling fin plates on the outer surface of the damper (either the housing or the cover side). The goal of the present investigation is to decide, whether the smaller gap-sizes improve or degrade the service life of the silicone oil and which side of the housing is suitable for mounting the cooling fin plate to hold the temperature of the visco-damper at a lower degree.

In terms of gap-sizes, the axial (X) and radial (Y) gap-sizes of the initial model (INIT1) are shown in Figure 3 (left). Besides keeping the design specifications, the operational temperature can be affected by the gap-sizes as the heat is generated in the silicone oil due to the dissipated energy and spread to the environment by heat transfer. The reduction of the distance between the inertia ring and housing (if the expected wet lubrication of surfaces is ensured) allows less amount of fluid stored in the damper and makes the oil film thinner. In case of the modified damper geometry (MOD1) (see Figure 3 (left)) the axial gap size (X) is reduced by 18.6% and the radial gap-size (Y) is decreased by 12.5% thus the amount of stored oil in the damper is reduced by 9.6%. Due to this modification, the oil content inside the damper is expected to store less amount of heat and keep the inner components at a comparatively lower temperature.

As far as cooling fin mounting is concerned, several cooling fin designs were tested previously, and it turned out that not the shape but the length, the height and the mounting position of the fins have a significant effect on the heat transfer process and thus on the cooling efficiency. [5] The initial model (INIT2) for mounting investigation with 'tunnel type' cooling fins assembled on the engine-side is shown in Figure 3 (right). In this case the gap-sizes remain unchanged. Considering the proximity of the engine and the heat transfer characteristics of the cooling fins, it would be advisable to relocate the fin plate onto the other side (free-side) of the damper housing.

As the damper rotates together with the engine crankshaft, free-stream of ambient air cools the fins more efficiently and more amount of heat can be discharged from the fins compared to the engine-side of the housing where the air close to the fins is rather stagnated with limited ventilation. Figure 3 (right) also shows the modified cooling fin mounting model (MOD2) for CFD investigation.

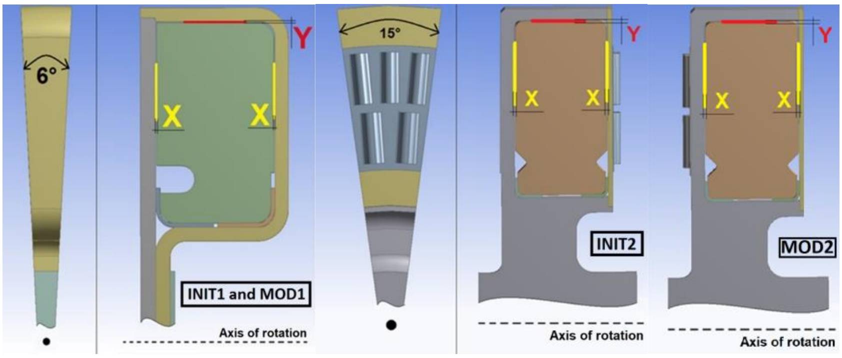

Figure 3
Initial and modified geometries for gap-size (left) and for mounting investigation (right)

To reduce the calculation time but maintain the accuracy of the results, only a sector of the whole damper-shaft-engine geometry is investigated considering the rotational periodicity. In case of gap-size simulations (INIT1 and MOD1) the investigated sector angle is $\beta_1 = 6°$ while in case of cooling fin mounting simulations (INIT2 and MOD2) a sector angle of $\beta_2 = 15°$ is considered. The greater β_2 provides enough width for fulfilling the periodicity conditions for the flow field including fins.

The geometries are prepared by Creo Parametric. The simplified geometries with the crankshaft, engine and flow fields are finalized in Ansys "Design Modeler" submodule. The slide bearings are removed since their effect on the oil has already been considered in the lifetime analysis. The housing and cover are merged (called case or casing in the following subchapters) because they are made of the same material and welded. The boundaries of the ambient are set far away from the investigated damper-shaft-engine system to protect it from the flow-disturbing effects of the structure.

3.2 Numerical Mesh

Generating mesh is the crucial part of numerical calculations. The smaller the mesh size, the more accurate the results would be, resulting in, however, a longer calculation time. Results can also be influenced by properly selecting and creating mesh elements. Hence, mesh size sensitivity and quality analysis has been completed to find the most suitable mesh configurations, keeping in mind the accuracy (maximum acceptable skewness, aspect ratio, etc.), the optimum cell number (for resolving heat transfer processes) and effort needed for mesh generation.

As denser mesh at the wall (or inflation layer) has a prominent role in modelling heat transfer processes accurately, preliminary calculations for Reynolds number, dynamic and kinematic viscosity, shear velocity, wall shear stress, skin friction coefficient, first cell height and the boundary layer thickness are determined and used as described in [30].

The final mesh, in case of INIT1 and MOD1, is built up from approximately 11 million elements, whereas, in the case of INIT2 and MOD2 (see Figure 4), the cell number is approximately 15 million. In each case the y+ (dimensionless distance from the wall) is less than 1 and the boundary layer is split up to 15 sublayers, resulting in the CFD software using „Near-Wall Model Approach" technique. In this approximation, the discretized form of the transport equations is solved directly till the wall and provide more accurate results unlike using logarithmic-based wall functions.

The surrounding of cooling fin plate is called fin-zone, where a finer mesh must be used to take full advantage of the wall resolving approach. This region of air moves together with the fin plate and forms a transition between the static ambient domain and the rotating fins.

3.3 Boundary Conditions and Program Settings

After importing the final mesh into Ansys CFX submodule, the next step is defining material properties, boundary conditions and solver settings.

Silicone oil and air gap (rotating volumes) in the damper are modelled as solid domains (with density, viscosity, specific heat, thermal conductivity and considering energy conservation law) for two reasons. On the one hand, the effect

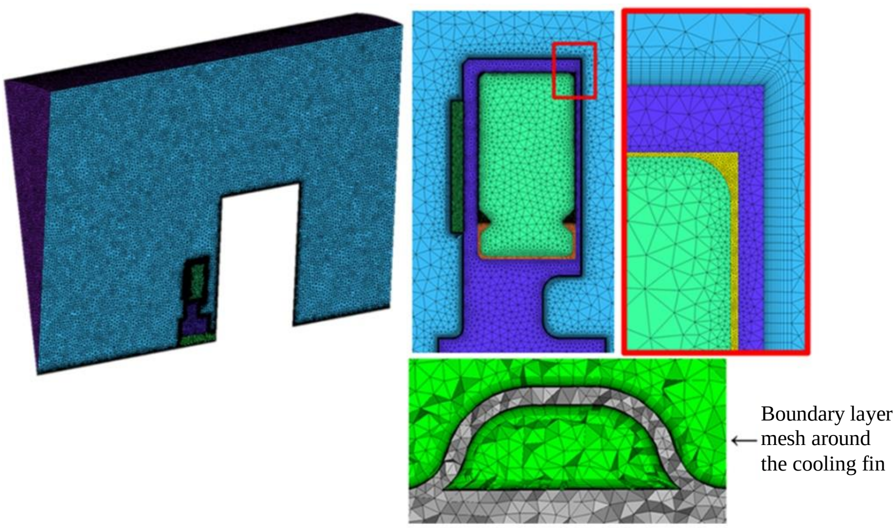

Figure 4
Numerical mesh (MOD2) with inflation layers for mounting investigation

of heat convection is negligible due to the rather stiff silicone oil at an elevated centrifugal force, thus heat can only be conducted as in a solid domain. On the other hand, calculating solid domain requires a shorter calculation time if the scope of the simulation is to determine the temperature distribution inside the damper. Shaft, case and ring (rotating solid domains) are defined with density, specific heat, thermal conductivity and with considering energy conservation law also. Ambient (stationary domain) and fin-zone (rotating domain) are set to flow domain with SST turbulence modelling, automatic wall function and with considering total energy conservation law. The applied material properties are found in Table 1.

Table 1

Materials and parameters used in the simulations

Material	**Air**	**Silicone fluid**	**Steel components**
Density [kg/m^3]	1.185	973	7854
Specific heat capacity [J/kg/K]	1004.4	550	434
Thermal conductivity [W/m/K]	0.0261	0.15	60.5

1500 RPM speed has been applied at silicone oil gap-size investigation and 1900 RPM is considered at cooling fin mounting investigation for the rotating domains.

The heat source (defined on the oil domain segment) is calculated by Eq. (3.1).

$$Q_V = \frac{Q_{damp}}{V^{oil} \cdot \frac{360°}{\beta}} \tag{3.1}$$

where Q_V is oil segment heat source [W/m^3]; Q_{damp} is damping performance [W]; V^{oil} is oil segment volume [m^3]; β is investigated sector angle [deg].

2000 W damping performance is considered at silicone oil gap-size investigation and 1000 W is at cooling fin mounting investigation.

Interface connections are defined between the adjacent surfaces of the relevant domains as follows. Each domain connecting with itself circumferentially has rotational periodicity interface; there is a heat resistance free contact between case and shaft; fin-zone has a rotating wall interface at the connection with ambient air while the shaft and case are in a rotating solid wall interface connection with the ambient air. Finally, perfect heat transfer interface is defined between fin-zone and case, oil and case, air gap and case, air gap and oil, oil and ring, and air gap and ring. These connections are shown in Figure 5 (right) for cooling fin mounting investigation.

The boundary conditions for cooling fin geometry investigation case are presented in Figure 5 (left). The ambient domain contains stationary walls (next to the surfaces of the engine with a constant temperature) and rotating walls (next to the surfaces of the damper, the fin-zone and the shaft). The far field surfaces of the ambient domain are set to be Opening (Entrainment) with constant static temperature 50° C, relative static pressure 0 bar and „Opening pressure and Direction" option.

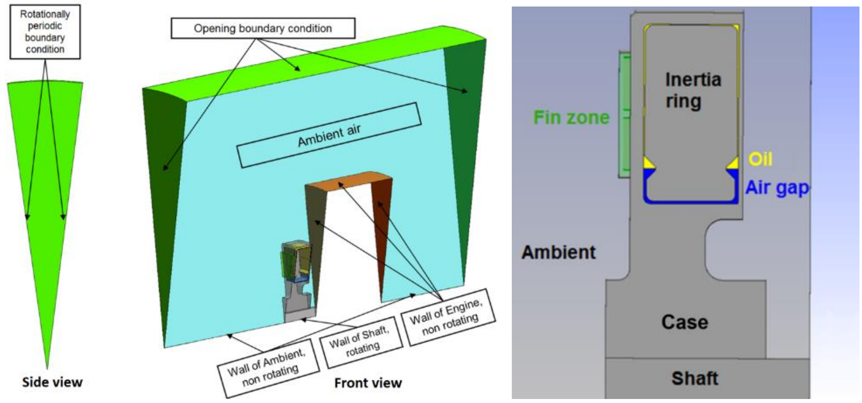

Figure 5

Boundary conditions (left) and interface connections (right) for mounting investigation

The turbulent intensity is set to be medium (5%). Nine monitoring points (in the function of radius) are defined on the casing to monitor the convergence of temperature and the area-averaged temperature during the numerical calculation. The last step is the solver settings in the software setup. 'High resolution' advection scheme is used, while turbulence numeric is defined to be 'First order'. The number of maximum allowed iteration steps is 5000.

Timescale control is specified by a timescale factor of 30 for fluid domains and 10 for solid domains. Convergence criteria are given by the residual target of RMS 10^{-6} and the conservation target of imbalances is 1%.

3.4 Evaluation of Numerical Results

3.4.1 Gap-Size Investigation

Figure 6 shows the convergence curves of temperatures at different monitoring points in case of INIT1 analysis. The graph proves the convergence; the constant temperatures are reached after 2500 iterations for INIT1. The convergence-increase around 1800^{th} iteration can be explained by the fact that the time scale factor in the solver has been changed to improve convergence and reduce the calculation time. The convergence is also reached for the MOD1 simulation after 1000 iterations. MOD1 simulation needed less iteration steps to reach convergence because of the fact, that the calculation has been initialized from the converged results of INIT1 simulation. In each analysis results the residuum reached the residual 10^{-4} and each imbalance goes below 1% conservation target at the end of the calculation.

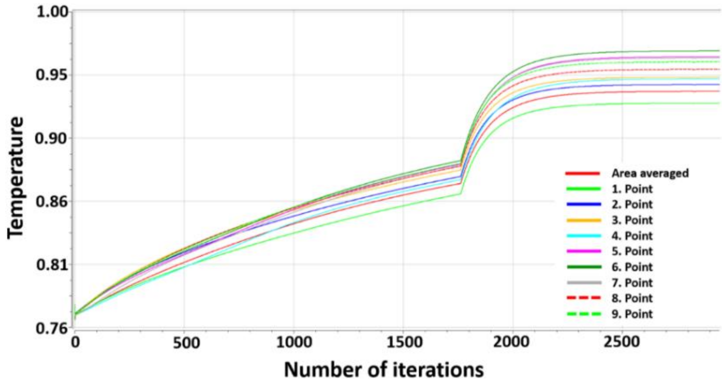

Figure 6
Temperature convergence of INIT1 analysis at gap-size investigation

Figure 7 shows the normalized temperature distribution in the dampers (on the left) and the heat flux on the outer side of the case (on the right) for INIT1 and MOD1. The outside area-averaged temperature of the case shows 1.7% difference from the pre-calculated value by Eq. (1.1) at the same conditions, thus the presented simulation results are plausible, and the simulation is suitable for further engineering purpose. The location of the heat source and a stagnant flow region of air between the engine and the damper can be identified in the left side of the figure. This latter region has poor cooling efficiency; the average temperature here is higher than the ambient temperature by 11.7%. That can be proven also by the intensity of heat transfer on the outer side of the case (see Figure 7 (right)). It turns out that the pattern of cooling intensities shows similarities for both geometries and they are the function of radius.

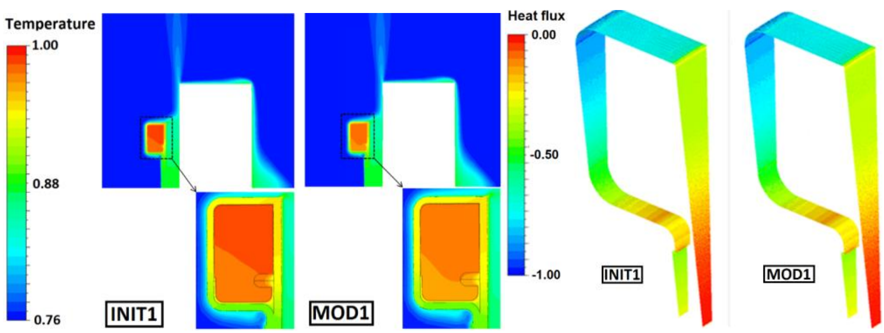

Figure 7
Normalized temperature distribution (left) and heat flux of the case (right) at gap-size investigation

Figure 8 shows the temperature distribution in the oil region for INIT1 (on the left) and for MOD1 (on the right) geometries. There is a difference on the inner side of the oil rings. In case of MOD1 geometry, the temperature is lower, and the peak temperature of the oil is less by 1% compared to the baseline geometry.

The temperature values of both oil domains have been exported and a *DF* value has been calculated for each exported temperature based on [20]. After averaging the gained *DF* values in both oil domains, the lifetime for each investigated case has been determined by Eq. 2.3. The results present that the suggested gap-size modification (corresponds to less amount of oil by 9.6%) causes a lifetime increment by 25.8% compared to the initial geometry (INIT1) on average.

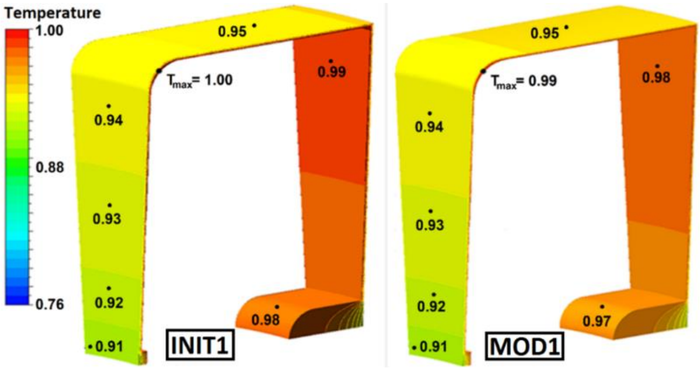

Figure 8
Temperature distribution in the oil rings at gap-size investigation

3.4.2 Cooling Fin Mounting Investigation

INIT2 and MOD2 simulations provided similar convergence curves to Figure 6. The calculation is converged for INIT2 when the constant temperatures are reached after 5000 and for MOD2 after 1400 iterations respectively. In both calculations the residuum reached 10^{-4} and each imbalance goes below 1% target at the end of the iteration steps.

Figure 9 shows the temperature distribution in the dampers (on the left) and the heat fluxes on the outer side of the case (on the right) for INIT2 and MOD2 variants. The outside area-averaged temperature of the case shows 2.6% difference from the pre-calculated value by Eq. (1.1), so the presented simulation results are suitable from plausibility point of view. The heat generation domain and the stagnant flow conditions between the damper and the engine are well visible also in the figure. Here, in this enclosed zone, the flow temperature is higher by 7.1% in average compared to the ambient temperature. The cooling fins show a poor cooling efficiency when they are mounted on the engine side. This can also be seen by the intensity of heat transfer on the outer side of the case (see Figure 9 (right)). The temperature varies along the radius of the case, from higher (near the center) to lower on the periphery, and hence, the cooling intensity can be determined to be a function of the radius of the case also. With the cooling fins mounted on the free side of the case, the overall temperature observed is lower as compared to when the cooling fins are situated on the engine side, so this variant has higher cooling efficiency.

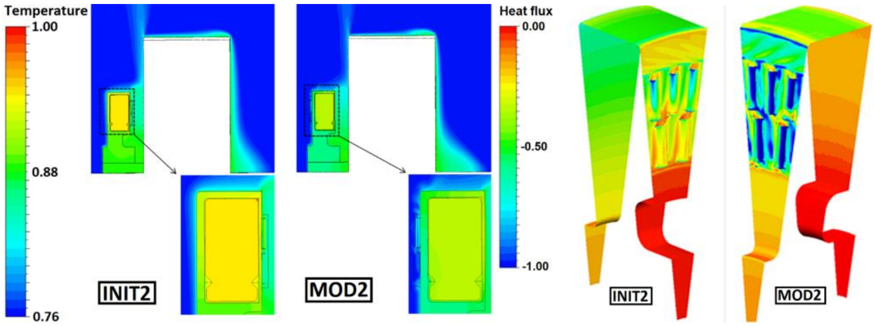

Figure 9

Normalized temperature distribution (left) and heat flux of the case (right) at cooling fin mounting investigation

Figure 10 shows the temperature distribution in the oil segment for INIT2 (on the left) and for MOD2 (on the right) geometries. There is a significant difference both on the outer and inner sides of the oil regions. In case of MOD2, not only the peak temperature of the oil is lower but the temperature distribution throughout the oil region is less compared to INIT2. Similarly, to the gap-size investigation case, the temperature values of both oil domains were exported and lifetime calculations were performed based on [20] with help of Eq. 2.3. It turned out that the suggested cooling fin mounting modification (MOD2) causes a lifetime increment of 133.2% in comparison with the initial geometry (INIT2).

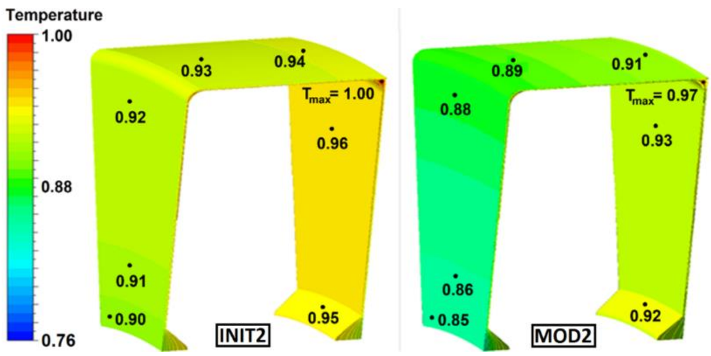

Figure 10

Normalized temperature distributions in the oil rings at cooling fin mounting investigation

Conclusions

Viscous torsional vibration dampers are essential accessories of high performance and/or downsized piston engines and are exposed to complex mechanical, thermal and chemical loads, within their componentry. The lifespan of visco-dampers is influenced, primarily, by the usage of its working medium, which is strongly affected by the operational temperature. Hence, it is always necessary, in the preliminary design phase, to properly estimate and control the oil temperature for slowing down the thermal degradation process. Analytical and numerical methods have been used in this work to determine the temperature distribution and its plausibility. Design modifications have been suggested and thoroughly analyzed, by coupled fluid dynamic and heat transfer simulations, to check their effect on the temperature and service life of the damping medium.

The influence of gap-sizes and positioning of the mounted cooling fins on the lifespan of the silicone oil, has been brought to light, with the help of CFD simulations. MOD1 geometry with smaller gap-sizes and lesser quantity of silicone oil by 9.6% provides longer lifespan by 25.8% compared to the original INIT1 geometry. The MOD2 geometry places the cooling fins on the free side, away from the engine, providing a lower temperature level and a lifetime is 2.33 times longer as compared to the INIT2 geometry.

The visco-damper technology depends strongly on the degradation properties of the silicone oil. Thus, the improvement of recently applied lifetime estimation method, is indispensable for increasing accuracy. Hence, the next step within the framework of the present study, is to update the available lifetime prediction method, by means of completing further degradation measurements, at lower operational temperatures. Future simulations are planned, including validation under different operational conditions, including advanced cooling fin geometries, to better understand and improve thermal behavior and therefore, the durability.

Acknowledgement

This work was supported by the Pro Progressio Foundation. We would like to express our special thanks to Sándor Kovács and Gábor Rácz from the Engineering Calculations Team at Knorr-Bremse R&D Center Budapest for their technical support in CFD. We would like to show appreciation to Mr. Shayan Asim at Hasse und Wrede GmbH in Berlin for his valuable help in revision and improvements the quality of the paper.

References

[1] Szalay, Zs., Tettamanti, T., Esztergár-Kiss, D., Varga, I. and Bartolini, C.: Development of a Test Track for Driverless Cars: Vehicle Design, Track Configuration, and Liability Considerations, Periodica Polytechnica Transportation Engineering, 46:(1), pp. 29-35, 2017, DOI: https://doi.org/10.3311/PPtr.10753

[2] Sándor, Z.: Effects of Weather Related Safety Messages on the Motorway Traffic Parameters, Periodica Polytechnica Transportation Engineering, 45:(2), pp. 58-66, 2017, DOI: https://doi.org/10.3311/PPtr.9117

[3] Érsek, P.: Numerische Untersuchung der Auffüllung eines Torsiondämpfers mit Silikonöl, Knorr-Bremse R&D Center Budapest, Technische und Wirtshaftwissenschaftliche Universität Budapest, Lehrstuhl für Hydrodynamische Systeme, Diplomarbeit, Budapest, 2008

[4] http://www.lezo.hu/szerkezettan/hajtas/motor/szerkezet/forgattyustengely/forgattyus-tengely.html (Accessed: 23.08.2017)

[5] Hafner, K. E., Maass, H.: Torsionsschwingungen in der Verbrennungskraftmaschine, Die Verbrennungskraftmaschine, Neue Folge, Band 4, Springer-Verlag Wien-New York, pp. 392, 1985

[6] http://www.hassewrede.de/media/pictures/produkte/vd_r6_nfz_510ps.jpg (Accessed: 23.08.2017)

[7] Homik, W.: Torsional vibration silencers used in vessels propulsion systems, Scientific Journals, 40:(112), pp. 9-16, 2014, ISSN 1733-8670

[8] Do-Kwan, H., Chan-Woo, A., Jae-Joon, S., Sang-Suk, L., Young-Duk, J.: Development and Experimental Performance Validation of Torsional Viscosity Damper for Crank Shaft System of Transporting Machine, International Journal of Precision Engineering and Manufacturing, 16:(7), pp. 1591-1597, 2015, DOI: https://doi.org/10.1007/s12541-015-0209-8

[9] Navale, V. R., Dr. Dhamejani, C. L.: Analysis of Damping Coefficient for Viscous Damper, International Journal of Innovations in Engineering Research and Technology, 2:(7), 2015, ISSN: 2394-3696

[10] Ehab, A., Rama, B., Ramin, S.: Development of a new torsional vibration damper incorporating conventional centrifugal pendulum absorber and magnetorheological damper, Journal of Intelligent Material Systems and Structures, 27:(7), pp. 980-992, 2015, DOI: https://doi.org/10.1177/1045389X15590275

[11] Anant, C., Nigam, S. P.: Magnetorheological Fluids in Viscous Friction Torsional Vibration Dampers, International Journal of Mechanical and Production Engineering, 3:(3), 2015, ISSN: 2320-2092

[12] https://en.wikipedia.org/wiki/Silicone_oil (Accessed: 23.08.2017)

[13] https://en.wikipedia.org/wiki/Polydimethylsiloxane (Accessed:23.08.2017)

[14] Kőkuti, Z., van Gruijthuijsen, K., Jenei, M., Tóth Molnár, G., Czirják, A., Kokavecz, J., Ailer, P., Palkovics, L., Völker, A. C., Szabó, G.: High-frequency rheology of a high viscosity silicone oil using diffusing wave spectroscopy, Applied Rheology, 24 (2014) 63984, 2014, DOI: http://doi.org/10.3933/ApplRheol-24-63984

[15] Kőkuti, Z., Völker-Pop, L., Brandstätter, M., Kokavecz, J., Ailer, P., Palkovics, L., Szabó, G., Czirják, A.: Exploring the nonlinear viscoelasticity of a high viscosity silicone oil with LAOS, Applied Rheology, 26 (2016) 14289, 2016, DOI: http://doi.org/10.3933/ApplRheol-26-14289

[16] Camino, G., Lomakin, S. M., Lazzari, M.: Polydimethylsiloxane Thermal Degradation Part 1, Kinetic Aspects, Polymer, 42:(2001), pp. 2395-2402, 2001, DOI: https://doi.org/10.1016/S0032-3861(00)00652-2

[17] Camino, G., Lomakin, S. M., Lazzari, M.: Polydimethylsiloxane Thermal Degradation Part 2, The Degradation Mechanism, Polymer, 43:(2002), pp. 2011-2015, 2002, DOI: https://doi.org/10.1016/S0032-3861(01)00785-6

[18] Dongzhi, C., Xiaoyun, H., Hongwei, Z., Xianze, Y., Yingshan, Z.: Preparation and Properties of Novel Polydimethylsiloxane Composites Using Polyvinylsilsesquioxanes as Reinforcing Agent, Polymer Degradation and Stability, 111, pp. 124-130, 2015, DOI: https://doi.org/10.1016/j.polymdegradstab.2014.10.026

[19] Wang, M., Zhou, R., Xu, X.: The Engine Silicone-oil Damper Matching Calculation Method Based on the Heat Balance, Research Journal of Applied Sciences, Engineering and Technology, 4:(16), pp. 2773-2777, 2012, ISSN: 2040-7467

[20] Érsek, P., Nagy, I., Kiss, Cs., Németh, H.: Silicone Oil Degradation Tests, Knorr-Bremse R&D Center Budapest, Internal Project Report, Budapest, 2014

[21] Bera, J., Pokorádi, L.: Monte-Carlo simulation of helicopter noise, Acta Polytechnica Hungarica, Vol. 12, No. 2, pp. 21-32, 2015

[22] Sziroczák, D., Jankovics, I., Gál, I., Rohács, D.: Conceptual design of small aircraft with hybrid-electric propulsion systems, Energy, Vol. 204, 2020, ISSN 0360-5442, https://doi.org/10.1016/j.energy.2020.117937

[23] Beneda, K.: Numerical Simulation of MEMS-based Blade Load Distribution Control in Centrifugal Compressor Surge Suppression, in ICNPAA 2012 Congress: Mathematical Problems in Engineering, Aerospace and Sciences, Vienna, Austria, 2012

[24] Beneda, K.: CFD Simulation of Blade Load Distribution Control as Active Centrifugal Compressor Surge Suppression, ACTA AVIONICA, Vol. 15, No. 25, pp. 13-20, 2013

[25] Bicsák, Gy., Veress, Á.: New Adaptation of Actuator Disc Method for Aircraft Propeller CFD Analyses, Acta Polytechnica Hungarica, 14:(6), pp. 95-114, 2017, DOI: https://doi.org/10.12700/APH.14.6.2017.6.6

[26] Kátai, L., Várszegi, T., Oldal I., Zsidai. L.: Hydrodynamic Modelling and Analysis of a New-Developed Mobile Refrigerated Container, Acta Polytechnica Hungarica, 13:(5), pp. 83-104, 2016, DOI: https://doi.org/10.12700/aph.13.5.2016.5.5

[27] Akbarian, E., Najafi, B., Jafari, M., Ardabili, S. F., Shamshirband, S., Chau, K. W.: Experimental and Computational Fluid Dynamics-Based Numerical Simulation of Using Natural Gas in a Dual-Fueled Diesel Engine, Engineering Applications of Computational Fluid Mechanics, 12:(1), pp. 517-534, 2018, DOI: https://doi.org/10.1080/19942060.2018.1472670

[28] Fabio, B., Giuseppe, C., Stefano, F.: A Modified Thermal Wall Function for the Estimation of Gas-To-Wall Heat Fluxes in CFD In-Cylinder Simulations of High Performance Spark-Ignition Engines, Applied Thermal Engineering, 115, pp. 1045-1062, 2017, DOI: https://doi.org/10.1016/j.applthermaleng.2017.01.055

[29] ANSYS, ANSYS CFX-Solver Theory Guide, Release 14.5, Southpointe, 275 Technology Drive, Canonsburg, PA 15317, 2012

[30] http://imechanica.org/files/fluent_13.0_lecture06-turbulence.pdf (Accessed: 17.09.2017)